PCCP

ROYAL SOCIETY OF CHEMISTRY

PAPER

View Article Online
View Journal | View Issue

Cite this: *Phys. Chem. Chem. Phys.*, 2020, **22**, 23207

Influence of linkage type (ether or ester) on the monolayer characteristics of single-chain glycerols at the air–water interface†

D. Vollhardt, *[a] B. Dobner[b] and G. Brezesinski[c]

O-1-Alkylglycerols are ubiquitous constituents in various biological materials but their biological significance is still largely unknown. So far, reports about the striking role of structural features on the interfacial properties of 1-*O*-alkylglycerol monolayers are quite rare. Therefore, in the present paper 1-*O*-alkylglycerol monolayers are comprehensively characterized on mesoscopic and molecular scales in the accessible ranges of temperature and surface pressure. Two Bragg peaks found for the condensed monolayer phase of the racemates at all pressures investigated indicate an orthorhombic structure with NN-tilted alkyl chains at lower pressures and NNN-tilted chains at higher pressures. In contrast to the continuous change of the tilt angle, as observed for many amphiphile monolayers, the tilt angle in 1-*O*-alkyl-*rac*-glycerol monolayers shows a jump-like transition from the L_2 (NN tilt direction) to the Ov phase (NNN tilt direction) with the consequence of different slopes of $1/\cos(t)$ *vs.* π in the two phases. This is the most striking difference to the behavior of the corresponding ester compound 1-stearoyl-*rac*-glycerol, having an oblique phase between the two orthorhombic phases L_2 and Ov at low temperatures. The generic phase diagrams of the 1-*O*-alkyl-*rac*-glycerol and 1-acyl-*rac*-glycerol monolayers are essentially different. The influence of chirality on the monolayer structure is weak and becomes even weaker at high temperatures (rotator phases) and high lateral compression. The GIXD results of the enatiomeric pure compounds show the expected oblique lattice structure characterized by three Bragg peaks at almost all lateral pressures measured. The results of the GIXD studies are complemented by other monolayer characteristics such as π–A isotherms and mesoscopic domain topographies. The π–A isotherms of 1-*O*-alkyl-*rac*-glycerols are similar to those of the corresponding 1-acyl-*rac*-glycerols indicating that the change from the ester linkage to the ether linkage does not affect significantly the thermodynamic features. However, pronounced differences in the topological structure are observed. 1-*O*-hexadecyl-*rac*-glycerol monolayers form three-armed domains whereby each arm is subdivided into two segments with different molecular orientation. Also fascinating chiral discrimination effects are observable, demonstrated in the case of S-enantiomers by always clockwise curved spirals at the domain periphery. The 1 : 1 racemic mixtures exhibit both clockwise and counterclockwise curved spirals.

Received 5th August 2020,
Accepted 22nd September 2020

DOI: 10.1039/d0cp04153j

rsc.li/pccp

Introduction

1-Substituted monoglycerols have been frequently studied in bulk and at the air–water interface. Therefore, amphiphilic monoglycerol monolayers have been investigated as model systems to characterize the striking role of the structural features on the interfacial properties. The effect of the chemical structure of the substituted polar group and its position at the glycerol backbone have been highlighted. As demonstrated, small changes in the polarity by refined variation in the head group structure affect impressively the mesoscopic structures in μ-range and the microscopic structure in Å-range. Such monolayer model systems are of relevance for better understanding the complex phenomena relating the functionality and activity of biological molecules and their potential application.[1–7] The comparison of four racemic amphiphilic monoglycerol types (amide, ether, ester and amine) has demonstrated how systematic alterations of the polar group structure and the corresponding changes in the dipolar interaction can drastically affect the shape

[a] *Max-Planck Institute for Polymer Research, Ackermannweg 10, D-55128 Mainz, Germany. E-mail: vollhardtd@mpip-mainz.mpg.de*
[b] *Institute of Pharmacy, Martin Luther University Halle-Wittenberg, Wolfgang-Langenbeck-Strasse 4, D-06120 Halle, Germany*
[c] *Institute for Applied Dermatopharmacy, Martin Luther University Halle-Wittenberg, Weinbergweg 23, D-06120 Halle, Germany*

† Electronic supplementary information (ESI) available. See DOI: 10.1039/d0cp04153j

of condensed phase domains.[8,9] The crystalline nature of the domains increases from amine having certain fluidity and fractal nature to amide having several orders of magnitude higher orientational correlation.[8]

So far, several monoacylglycerol-containing biological systems have been found and studied, and monoacylglycerols have been employed in various products.[10,11] Due to the omnipresent occurrence of palmitoyl- and stearoylglycerol in biological and applied systems[12–14] their monolayers are the most examined. The obtained results have shown that knowledge of the interfacial characteristics is significant for various applications. In addition, 1-*O*-alkylglycerols are present in various biological materials.[15–17] They are ubiquitous constituents of animal cells, of mammalian tissues, and of several microorganisms. All naturally occurring glyceryl monoethers are *S*-enantiomers, but their biological significance is still largely unknown. So far, reports about the characteristics of 1-monoalkylglycerol monolayers are quite rare, although first comparative monolayer studies of 1-glyceryl monoethers and 1-glyceryl monoesters have shown some similarities of the thermodynamic features.[18,19]

Extensive studies of interfacial characteristics of 1-*O*-alkylglycerol monolayers should help to obtain more information for conclusions about specific phenomena that are of special interest in understanding inherent biological and technological processes.

In the present paper, 1-*O*-alkylglycerol monolayers are comprehensively characterized on mesoscopic and molecular scales in the accessible ranges of temperature and surface pressure. The thermodynamic analysis based on the π–A isotherms and the mesoscopic domain topography complements the characteristic features. Finally, the effect of chirality on the characteristic features of glycerolether monolayers is studied.

Experimental

The synthesis of 1-*O*- and 3-*O*-hexadecyl-*sn*-glcerol was carried out based on previous work.[20,21] In contrast to the methods of Bauman and Mangold[20] and Paltauf and Hermetter.[21] potassium hydride was used as the base and toluene as the solvent. Starting material was optical pure 2,3-*O*-isopropylidene-*sn*-glycerol and 1,2-*O*-isopropylidene-*sn*-glycerol which were purchased from Aldrich. Hexadecyl bromide was used as the alkylating agent. Both the alkylation and the cleavage of the isopropylidene protecting group took place under conditions free of racemization. To remove the IP protective group, pyridinium tosylate in methanol was used in a neutral environment. Experimental details to the alkylation reaction for 1-*O*-hexadecyl-2,3-*O*-isopropylidene-*sn*-glycerol (**1a**) and 3-*O*-hexadecyl-1,2-*O*-isopropylidene-*sn*-glycerol (**1b**), the following hydrolysis and the corresponding analytical data are presented in the ESI† (SI1). A self-made computer-interfaced film balance was used to measure the surface pressure–molecular area (π–A) isotherms. Using the Wilhelmy method with a roughened glass plate the isotherms were measured at a compression rate of ≤ 10 Å^2 (molecule min)$^{-1}$ with an accuracy of the surface tension of ± 0.1 mN m^{-1} and the molecular area of ± 0.5 Å^2. A Brewster angle microscope (BAM1 +, NFT, Gottingen, Germany) with the lateral resolution of ~ 4 μm was mounted at the experimental setup. Comprehensive information about the BAM method is given elsewhere (see *e.g.* ref. 22–24).

The lateral structures of the monolayer at the air/water interface were investigated using grazing incidence X-ray diffraction (GIXD) measurements at the BW1 beam line, HASYLAB (Hamburg, Germany). A monochromatic X-ray beam ($\lambda = 1.304$ Å) strikes the water surface at a grazing incidence angle $\alpha_i = 0.85\alpha_c$ (where $\alpha_c = 0.13^\circ$ is the critical angle for total reflection of the X-ray beam at the water surface) illuminating approximately 2×50 mm^2 monolayer surface in a thermostated Langmuir film balance placed in a hermetically closed container filled with helium. During the run of the experiment, a slow lateral movement of the trough is used in order to avoid sample damage by the strong X-ray beam.

A linear position-sensitive detector (PSD, OEM-100-M, Braun, Garching, Germany) measured the diffracted signal and was rotated to scan the in-plane Q_{xy} component values of the scattering vector. The vertical channels of the PSD measured the out-of-plane Q_z component of the scattering vector between 0 and 0.85 Å^{-1}.

The Bragg peaks, obtained by integration of the scattering intensity (corrected for polarization, effective area, and Lorentz factor) over a certain Q_z window, and the Bragg rods, obtained by the integration of the scattering intensity over a certain Q_{xy} window, give information about the unit cell dimensions. The in-plane lattice repeat distances, d, of the ordered structures in the monolayer were calculated from the Bragg peak positions: $d = 2\pi/Q_{xy}$. The extent of the crystalline order in the monolayer, the in-plane coherence length L_{xy}, can be approximated from the full-width at half-maximum (fwhm) of the Bragg peaks using $L_{xy} \sim 0.9(2\pi)/\mathrm{fwhm}(Q_{xy})$. The thickness of the scattering unit can be estimated from the fwhm of the Bragg rod using $0.9(2\pi)/\mathrm{fwhm}(Q_z)$. More details can be found in the literature.[25–28]

Results and discussion

The π–A isotherms of 1-*O*-hexadecyl-*rac*-glycerol and 1-*O*-octadecyl-*rac*-glycerol monolayers on water have been measured at different temperatures in the range between 10 and 40 °C (Fig. 1). The features of the π–A isotherms are comparable to those of the most usual amphiphiles. The main phase transition between a fluid (gaseous, G; liquid-expanded, LE) and a condensed (LC) phase is a first-order transition characterized by a plateau in which the two phases co-exist. The transition pressure of the G-LC transition is close to zero and practically not depending on the temperature. In contrast, the LE-LC transition pressure is strongly temperature dependent. The results show that π–A isotherms of 1-*O*-alkyl-*rac*-glycerols are similar to that of the corresponding 1-alkanoyl-*rac*-glycerols indicating that the change from the ether linkage to the ester linkage does not affect significantly the thermodynamic features.

The π_t–T (Fig. 2) of 1-*O*-hexadecyl-*rac*-glycerol can be approximated with a linear relationship and a slope $\mathrm{d}\pi_t/\mathrm{d}T$ of 0.831 mN (m K)$^{-1}$

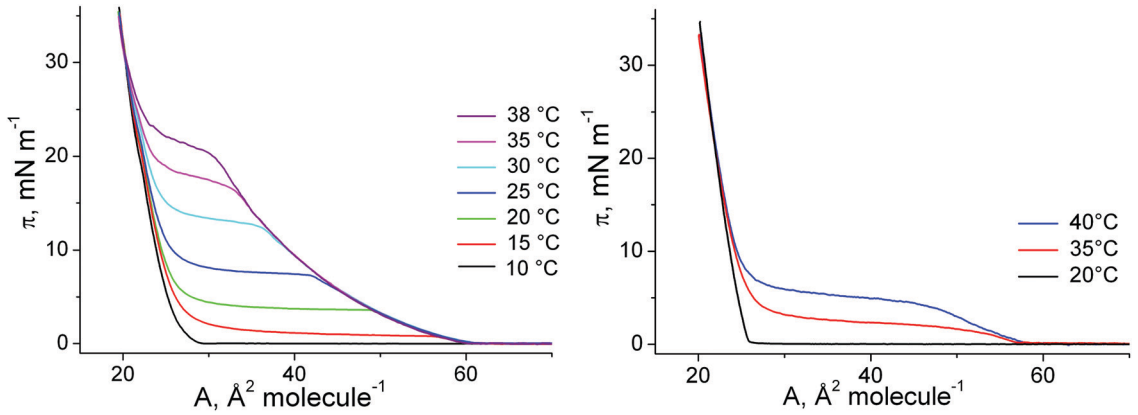

Fig. 1 π–A isotherms of 1-*O*-hexadecyl-*rac*-glycerol (left) and 1-*O*-octadecyl-*rac*-glycerol (right) at different temperatures (indicated).

yielding a T_0 of 288.4 K (15.2 °C). Above T_0, a nearly horizontal plateau region is observed, which is gradually more inclined at higher temperatures (above 30 °C). Comparing the isotherms of the C16- with those of the C18-compound suggests that the experimental temperature of the C16-compound has to be shifted by 19 degrees (~9 K per CH_2 group) to be comparable with the C18-compound in a generic phase diagram. This value is in good agreement with those described as 5 to 10 °C per additional methylene group for other amphiphilic monolayers.

The extension of the phase transition region of the 1-*O*-hexadecyl-*rac*-glycerol monolayers decreases in the usual way as the temperature increases. The entropy change $\Delta S = \Delta H/T$ of the phase transition was calculated using the two-dimensional Clapeyron equation $\left(\Delta H = (A_c - A_e)T\frac{d\pi_t}{dT}\right)$ with A_e – the molecular area at the onset of the phase transition at the surface pressure π_t and A_c – the area of the respective condensed phase at the same pressure. The temperature dependence of the entropy change ΔS yields the critical temperature of T_c = 318.1 K (44.9 °C), above which the monolayer cannot exist in the condensed state (Fig. 2, right).

In Fig. 2, the π_t and ΔS values of the ether compound 1-*O*-hexadecyl-*rac*-glycerol have been compared with those of the ester compound 1-palmitoyl-*rac*-glycerol. The corresponding thermodynamic data of ester and ether compounds are only marginally different (T_0 = 290.3 K, T_c = 322.4 K and T_0 = 288.4 K, T_c = 318.1 K, respectively) showing that the type of linkage of the hydropbobic chain to the glycerol unit has not much influence on the thermodynamics of the 2D system.

Despite similar thermodynamic features of 1-*O*-alkyl-*rac*-glycerols and 1-alkanoyl-*rac*-glycerols with the same chain length, pronounced differences in the morphological structure and the phase behavior are observed by BAM. The comparison of condensed phase domains of 1-*O*-hexadecyl-*rac*-glycerol and 1-palmitoyl-*rac*-glycerol demonstrates striking topographical differences (Fig. 3). The 1-*O*-hexadecyl-*rac*-glycerol monolayers form three-armed domains in the plateau region after the main phase transition. Each arm is subdivided into two segments with different molecular orientation. On the other hand, equilibrium 1-monopalmitoyl-*rac*-glycerol domains are subdivided into seven segments meeting in the center with jump-like change of orientation.

The GIXD experiments were carry out over a large range of lateral pressures at different temperatures (5, 10, 15 and 20 °C). Fig. 4 presents selected contour plots obtained for the racemates at 10 °C and 10 mN m^{-1} (bottom) and 30 mN m^{-1} (top).

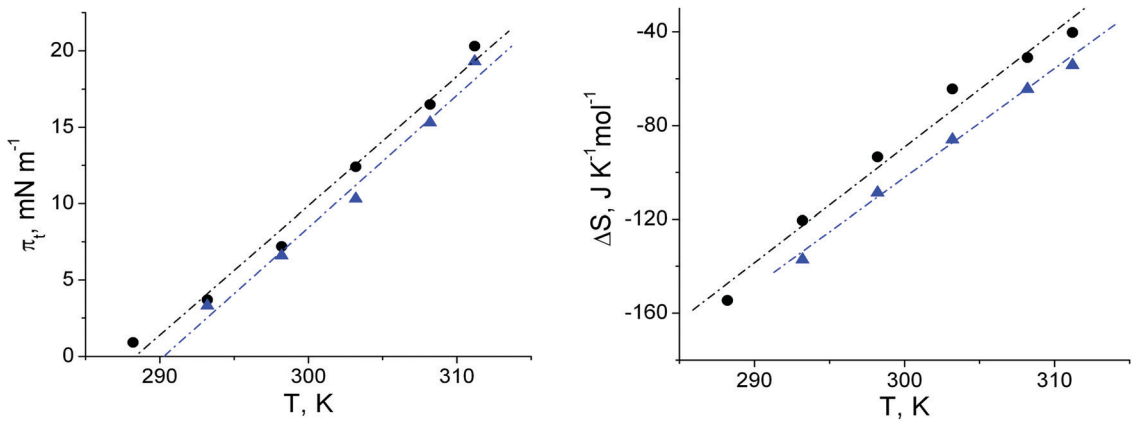

Fig. 2 Temperature dependence of the main phase transition pressure π_t (left) and of the entropy change ΔS (right) at the LE/LC phase transition of 1-*O*-hexadecyl-*rac*-glycerol (●) and 1-palmitoyl-*rac*-glycerol (▲) monolayers spread on water.

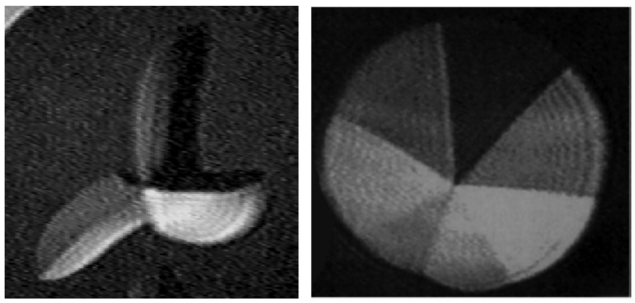

Fig. 3 Examples for the mesoscopic topography of equilibrium domains using BAM1+. (left) 1-*O*-Hexadecyl-*rac*-glycerol domain forming three-armed structures where each arm is divided into two segments of different orientation, (right) 1-monopalmitoyl-*rac*-glycerol domain subdivided into seven segments meeting in the center; T = 23 °C.

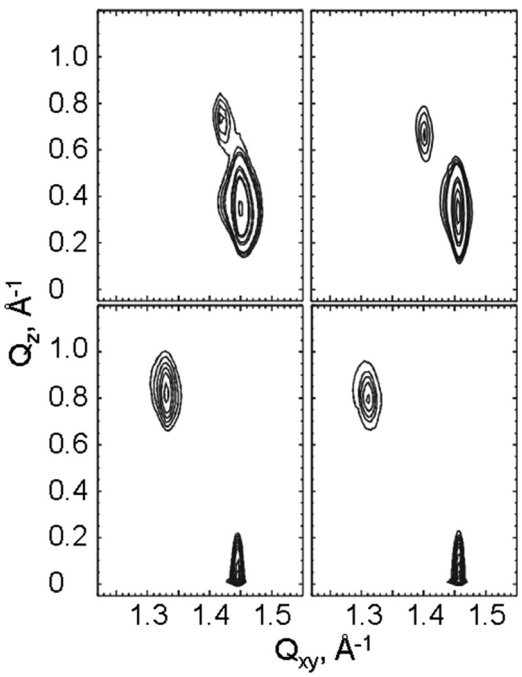

Fig. 4 From left to right: GIXD data of 1-*O*-octadecyl-*rac*-glycerol and 1-*O*-hexadecyl-*rac*-glycerol monolayers on water at 10 °C, measured at 10 mN m^{-1} (lower row) and 30 mN m^{-1} (upper row). The diffracted intensities, corrected for polarization, effective area, and Lorentz factor, are plotted as contour lines of equal intensity *vs.* the in-plane component Q_{xy} and the out-of-plane component Q_z of the scattering vector.

For all pressures, the diffracted intensity is plotted as contour lines of equal intensity *versus* the in-plane component Q_{xy} and the out-of-plane component Q_z of the scattering vector. The two Bragg peaks indicate that the condensed monolayer phase of the racemates has an orthorhombic structure in the whole pressure region. At lower pressures, the alkyl chains are tilted toward their nearest-neighbors (NN) with Bragg rods at $Q_z = 0$ and $Q_z > 0$. On compression, the tilt direction changes to NNN (next-nearest neighbors) indicated by the fact that both Bragg rods are at $Q_z > 0$.

The Bragg peak positions, their full-widths at half-maximum and all lattice parameters obtained at different surface pressures and different temperatures are listed in Tables S1–S24 (ESI†).

The cross-sectional area, A_0, of the racemates is, as expected, affected by the temperature and amounts to values between 19.5 (1-*O*-octadecyl-*rac*-glycerol at 5 °C) and 19.9 Å^2 (1-*O*-hexadecyl-*rac*-glycerol at 10 °C). In average, A_0 increases by 0.15 Å^2 with increasing the temperature by 10 K. These changes are similar to those observed with other amphiphiles. At low temperatures, the rotational freedom of the chains is drastically hindered while at higher temperatures typical values of rotator phases are observed.

The tilt angle t decreases with increasing pressure. The transition pressure into a non-tilted state can be determined by plotting of $1/\cos(t)$ as a function of the lateral pressure assuming a constant cross-sectional area along the isotherm.[29,30] Fig. 5 shows that the non-tilted state can be expected only at high lateral pressures above 50 mN m^{-1}. In contrast to all our other experiments with amphiphile monolayers, the tilt angle does not change continuously at low temperatures as it does at higher temperatures, but rather exhibits a jump during the transition from the L_2 (NN tilt direction) to the Ov phase (NNN tilt direction). Therefore, the slope of $1/\cos(t)$ *vs.* π is different in the two phases. Based on the different slope in the Ov phase, the transition pressure into the non-tilted state is much higher (Fig. 5 middle and right) compared with the values obtained by the linear fit using all data points (Fig. 5 left).

This observation is the most striking difference compared with the behavior of the corresponding ester compound stearoyl-*rac*-glycerol, for which an oblique phase has been observed at low temperatures between the two orthorhombic phases L_2 and Ov. In the present case, the surprising behavior of $1/(\cos t)$ *vs.* π at low temperatures is connected with a co-existence of L_2 and Ov over a small pressure range (Fig. 6).

For a better visualization of this co-existence between L_2 and Ov, the Bragg peaks, the Bragg rods and surface plots are presented in the ESI† (S25 and S26). The phase transition between 13 mN m^{-1} and 15 mN m^{-1} from NN to NNN tilted orthorhombic unit cell and the co-existence of both phases at 14 mN m^{-1} are clearly seen. This co-existence of the two orthorhombic phases must be connected with a change in the order of this phase transition. Usually, transitions between condensed phases are of second-order. Here, we have to assume a first-order phase transition, which must be weak because it is not connected with a clear plateau region in the isotherm (see Fig. S27, ESI†). However, the isotherm measured at 5 °C shows distinct features resembling a weak first-order transition in the pressure range where the co-existence of L_2 and Ov is observed in the GIXD experiments. In contrast, the isotherm measured at 20 °C exhibits a homogeneous pressure increase during compression (see Fig. S27, ESI†).

Generic phase diagrams can be obtained by systematically shifting the temperature axis by a certain value per additional methylene group.[31] In the present case, we can compare the first-order phase transition between the liquid and the condensed phases. Doing so, one has to shift the temperature axis of the C16-compound by 19 degrees. Therefore, the phase

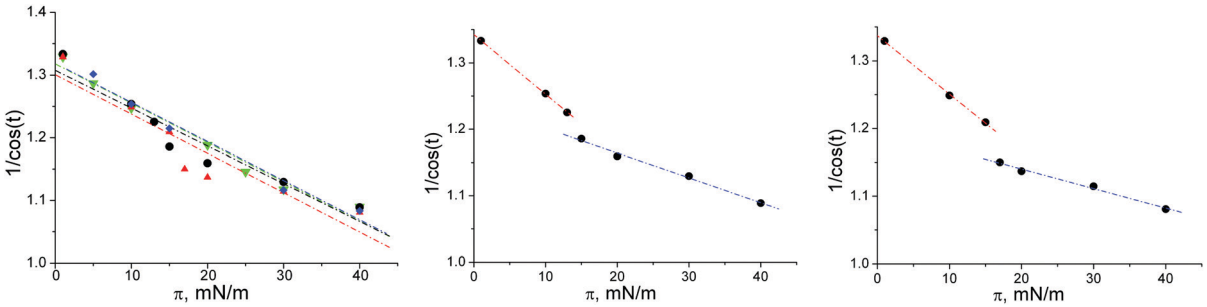

Fig. 5 $1/(\cos t)$ as function of the lateral pressure π of 1-*O*-octadecyl-*rac*-glycerol at ● – 5 °C, ▲ – 10 °C, ▼ – 15 °C, ◆ – 20 °C (left). The linear extrapolation toward zero tilt angle ($1/(\cos t) = 1$) yields the pressure of the tilting transition. Middle: $1/(\cos t)$ as function of the lateral pressure π of 1-*O*-octadecyl-*rac*-glycerol at 5 °C, right: at 10 °C, different slopes are observed in the L_2 and Ov phases.

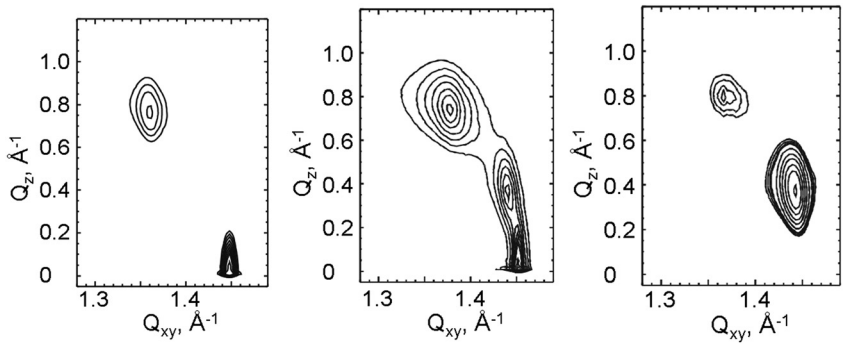

Fig. 6 GIXD data of 1-*O*-octadecyl-*rac*-glycerol monolayers on water at 5 °C, measured at 13 mN m^{-1} (left), 14 mN m^{-1} (middle) and 15 mN m^{-1} (right). The diffracted intensities, corrected for polarization, effective area, and Lorentz factor, are plotted as contour lines of equal intensity *vs.* the in-plane component Q_{xy} and the out-of-plane component Q_z of the scattering vector.

diagram of 1-*O*-hexadecyl-*rac*-glycerol monolayers has been shifted by 19 K and combined with that of 1-*O*-octadecyl-*rac*-glycerol. The generic phase diagram of 1-*O*-alkyl-*rac*-glycerol monolayers is shown in Fig. 7 and compared with that of 1-*O*-acyl-*rac*-glycerol monolayers. The most distinct differences are (i) the oblique phase between the two rectangular phases observed in monoacyl-*rac*-glycerol monolayers in contrast to the coexistence of the two rectangular phases in a small pressure range observed in monoalkyl-*rac*-glycerol monolayers, and (ii) the completely different temperature behavior of the L_2-Ov phase transition line which is strong for the acyl-*rac*-glycerol monolayers and almost non-existent for the alkyl-*rac*-glycerol monolayers.

Additionally, the effect of chirality on the thermodynamic behavior, topological features, and the 2D lattice structures of

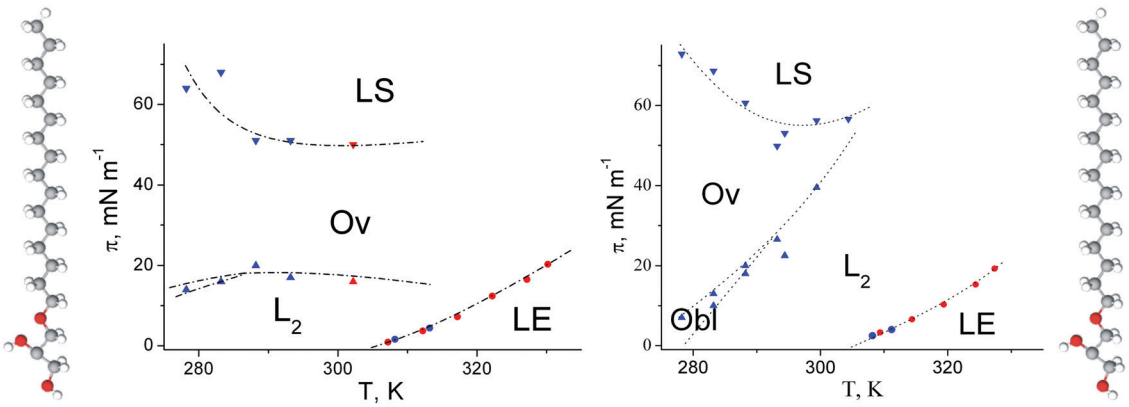

Fig. 7 Left: Generic lateral pressure–temperature phase diagram of the racemic 1-*O*-alkylglycerol monolayers on water. The temperature axis of the phase diagram of 1-*O*-hexadecyl-*rac*-glycerol (red labels) has been shifted by 19 K to match the phase diagram of 1-*O*-octadecyl-*rac*-glycerol (blue labels). Right: Generic lateral pressure–temperature phase diagram of the racemic 1-alkanoyl glycerol monolayers on water. The corresponding chemical structures of the molecules are presented.

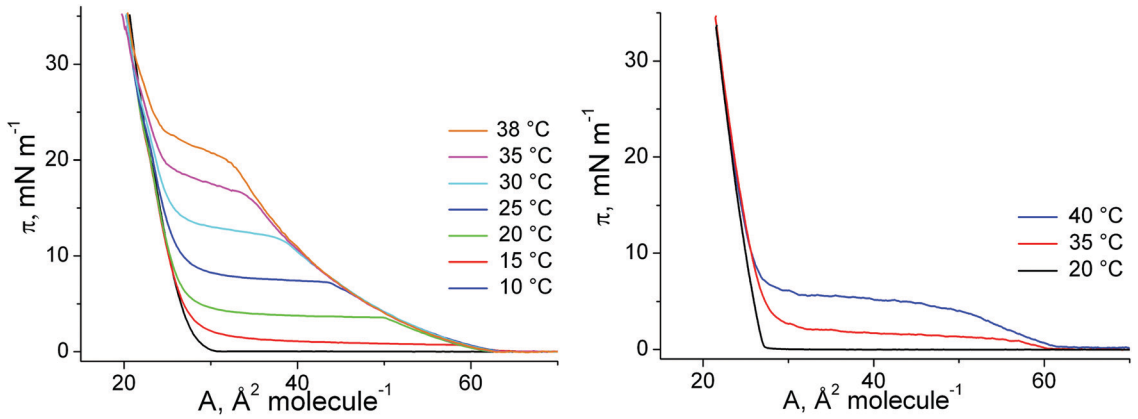

Fig. 8 π–A isotherms of 1-*O*-hexadecyl-*sn*-glycerol (left) and 1-*O*-octadecyl-*sn*-glycerol (right) at different temperatures (indicated).

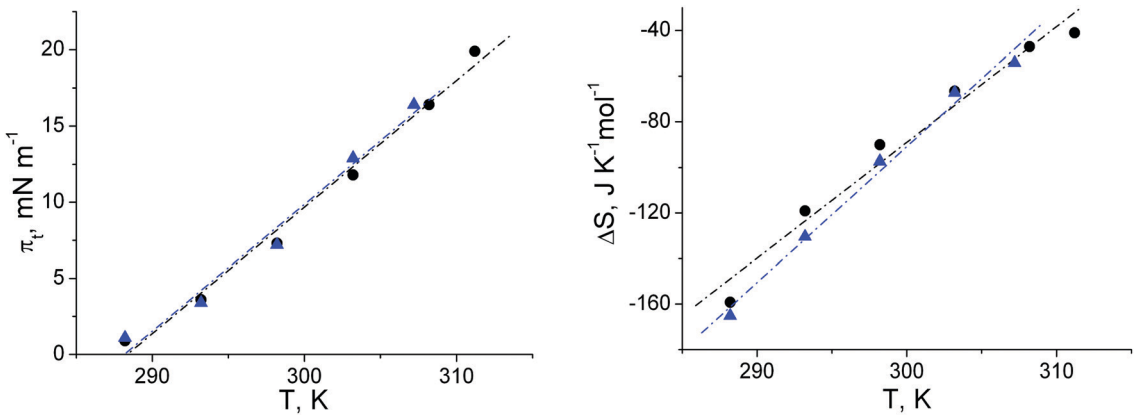

Fig. 9 Temperature dependence of the main phase transition pressure π_t (left) and of the entropy change ΔS (right) at the LE/LC phase transition of 1-*O*-hexadecyl-*sn*-glycerol (●) and 1-monopalmitoyl-*sn*-glycerol (▲) monolayers spread on water.

ether-glycerol monolayers has been studied. The surface pressure–area (π–A) isotherms (Fig. 8) are very similar to those reported for the racemates indicating that the influence of chirality is weak.

The extrapolated thermodynamic parameters (Fig. 9) are very similar to the ones of the racemates described above: 1-hexadecyl-*sn*-glycerol (T_0 = 288.4 K, T_c = 317.5 K) and 1-palmitoyl-*sn*-glycerol (T_0 = 288.2 K, T_c = 315.2 K). Also in the case of the enantiomeric pure compounds, the type of linkage of the hydropbobic chain to the glycerol unit has practically no influence on the thermodynamics of the 2D system.

1-*O*-Hexadecylglycerol monolayers show fascinating chiral discrimination effects (Fig. 10). In the case of *S*-enantiomeric 1-*O*-hexadecylglycerol monolayers, the spirals formed at the domain periphery are always clockwise curved whereas the monolayers of the 1 : 1 racemic mixtures are both clockwise and counterclockwise curved.[32] The oppositely curved spirals in the 1 : 1 racemic mixed monolayers suggest apparently chiral segregation of the two enantiomeric forms. These interesting experimental results about chiral discrimination effects in 1-*O*-hexadecyl glycerol monolayer initiated a theoretical work based on a coarse-grained molecular model. The study revealed an interesting crossover from heterochiral to homochiral preference.[33]

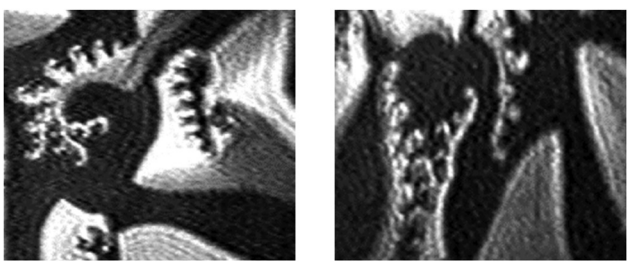

Fig. 10 Chiral discrimination in 1-*O*-hexadecylglycerol domains, T = 23 °C, $A \sim 0.3$ nm^2 per molecule: (left) *S*-enantiomer having always clockwise curved spirals, (right) racemic mixture with curvatures of the spirals in two opposite directions.

Due to the chiral nature of the enatiomeric pure compounds, the GIXD experiments show the expected oblique lattice structure characterized by three Bragg peaks at almost all lateral pressures measured (Fig. 11).

The exception is the shorter-chain compound 1-hexadecyl-*sn*-glycerol, which is comparable with 1-octadecyl-*sn*-glycerol measured at higher temperatures. As can be seen in the Tables S3–S8 (ESI†), the diffraction patterns at high lateral pressures can be described by two Bragg peaks typical for a

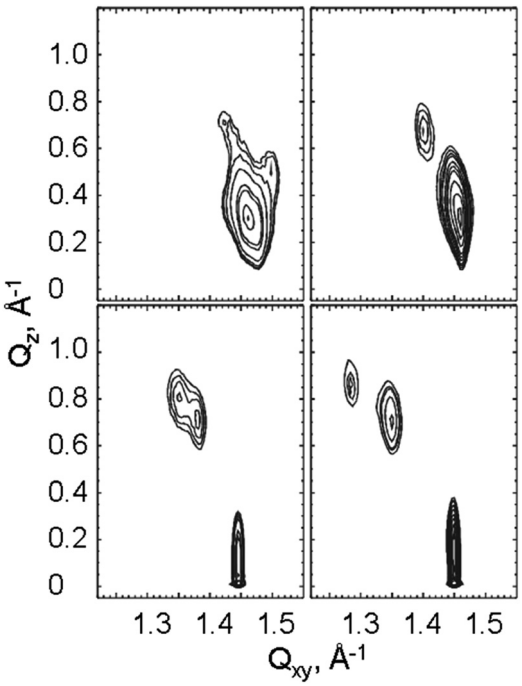

Fig. 11 From left to right: GIXD data of 1-*O*-octadecyl-*sn*-glycerol and 1-*O*-hexadecyl-*sn*-glycerol monolayers on water at 10 °C, measured at 10 mN m^{-1} (lower row) and 30 mN m^{-1} (upper row). The diffracted intensities, corrected for polarization, effective area, and Lorentz factor, are plotted as contour lines of equal intensity *vs.* the in-plane component Q_{xy} and the out-of-plane component Q_z of the scattering vector.

NNN tilted orthorhombic structure. This shows that chirality has a quite weak influence on the monolayer structure, and this influence becomes even weaker at high temperatures (rotator phases) and high lateral compression.

Conclusions

1-Substituted amphiphilic monoglycerol monolayers have been frequently investigated as model systems to characterize the striking role of structural features on the interfacial properties. The results of previous studies have highlighted that small changes of the chemical structure of the substituted polar groups affect impressively the mesoscopic structures in μm-range and the microscopic structure in nm-range. However, so far reports about the characteristics of 1-*O*-alkylglycerol monolayers are quite rare. Therefore, in the present paper 1-*O*-alkylglycerol monolayers are comprehensively characterized on mesoscopic and molecular scales in the accessible ranges of temperature and surface pressure.

The π–A isotherms of 1-*O*-alkyl-*rac*-glycerols are similar to those of the corresponding 1-acyl-*rac*-glycerols indicating that the change from the ester linkage to the ether linkage does not significantly affect the thermodynamic features. Comparing the temperature behavior of π–A isotherms of the C16- with those of the C18-compound implies a shift of 19 degrees (~9 K per CH_2 group) to be comparable in a generic phase diagram. The π_t–T of 1-*O*-hexadecyl-*rac*-glycerol approximated with a linear relationship and a slope $d\pi_t/dT$ of 0.831 mN (m·K)$^{-1}$ yields a T_0 of 288.4 K (15.2 °C). The critical temperature T_c = 318.1 K (44.9 °C), above which the monolayer cannot exist in the condensed state, results from the temperature dependence of the entropy change ΔS. Despite the similar thermodynamic features of 1-*O*-alkyl-*rac*-glycerols and 1-acyl-*rac*-glycerols with the same alkyl chain length, pronounced differences in the topological structure are observed by BAM. 1-*O*-Hexadecyl-*rac*-glycerol monolayers form three-armed domains in the plateau region after the main phase transition. Each arm is subdivided into two segments with different molecular orientation.

The GIXD experiments were performed over a large range of lateral pressures at different temperatures. Two Bragg peaks obtained for the condensed monolayer phase of the racemates over the whole pressure region indicate an orthorhombic structure with NN-tilted alkyl chains at lower pressures and NNN-tilted chains at higher pressures.

In contrast to other amphiphile monolayers, the tilt angle does not change continuously, but rather exhibits a jump during the transition from the L_2 (NN tilt direction) to the Ov phase (NNN tilt direction). Therefore, the slope of $1/\cos(t)$ *vs.* π is different in the two phases. This observation is the most striking difference compared with the behavior of the corresponding ester compound 1-stearoyl-*rac*-glycerol, for which an oblique phase has been observed at low temperatures between the two orthorhombic phases L_2 and Ov. The surprising behavior of $1/(\cos t)$ *vs.* π at low temperatures is connected with the co-existence of L_2 and Ov over a small pressure range resembling a weak first-order transition.

The generic phase diagrams of the monoalkyl-*rac*-glycerol and monoacyl-*rac*-glycerol monolayers show clear differences: (i) the oblique phase between the two rectangular phases observed in monoacyl-*rac*-glycerol monolayers is replaced by a coexistence of the two rectangular phases in a small transition range observed in monoalkyl-*rac*-glycerol monolayers, and (ii) the completely different temperature behavior of the L_2-Ov phase transition line.

The effect of chirality on the thermodynamic behavior, topological features, and the 2D lattice structures of ether-glycerol monolayers has been studied. The influence of chirality on the thermodynamics of the 2D system is weak. However, 1-*O*-hexadecylglycerol monolayers show fascinating chiral discrimination effects, demonstrated in the case of *S*-enantiomers by always clockwise curved spirals at the domain periphery and for the 1 : 1 racemic mixtures by both clockwise and counter-clockwise curved spirals.

The GIXD results of the enantiomeric pure compounds show the expected oblique lattice structure characterized by three Bragg peaks at almost all lateral pressures measured. However, chirality has a quite weak influence on the monolayer structure, it becomes even weaker at high temperatures (rotator phases) and high lateral compression.

Conflicts of interest

There are no conflicts to declare.

Acknowledgements

D. V. acknowledges the versatile assistance by Prof. Hans-Jürgen Butt. We thank HASYLAB at DESY (Hamburg, Germany) for beamtime and excellent support, and Irina Berndt (Max Planck Institute of Colloids and Interfaces, Potsdam, Germany) for careful Langmuir isotherm experiments. Open Access funding is provided by the Max Planck Society.

References

1 J. J. Ramsden, *R. J. Mol. Rec.*, 1997, **10**, 109–120.
2 P. C. Hiemenz, *Principles of colloid and surface chemistry*, Marcel Dekker Inc., New-York, 1997.
3 K. Holmberg, D. O. Shah and M. J. Schwuger, *Handbook of Surface and Colloid Chemistry*, New-York, Wiley, 2002.
4 M. C. Moran, A. Pinazo, L. Perez, P. Clapes, M. Angelet, M. T. Garcia, M. P. Vinardell and M. R. Infante, *Green Chem.*, 2004, **6**, 233–240.
5 I. Kuzmenko, H. Rapaport, K. Kjaer, J. Als-Nielsen, I. Weissbuch, M. Lahav and L. Leiserowitz, *Phys. Chem. Chem. Phys.*, 2001, **101**, 1659–1696.
6 A. Kumar, H. A. Biebuyk and G. M. Whitesides, *Langmuir*, 1994, **10**, 1498–1511.
7 M. Ramanathan, L. K. Shrestha, T. Mori, Q. Ji, J. P. Hill and K. Ariga, *Phys. Chem. Chem. Phys.*, 2013, **15**, 10580–10611.
8 D. Vollhardt, Surfactant Monolayers, in *Encyclopedia of Colloid and Interface Science*, ed. T. Tadros, Springer-Verlag, Berlin, Heidelberg, 2013, pp. 1165–1201.
9 N. Nandi and D. Vollhardt, *Acc. Chem. Res.*, 2007, **40**, 351–360.
10 H. Moonen and H. Bas, Mono- and diglycerides, in *Emulsifiers in food technology*, ed. R. J. Whitehurst, Blackwell Publishing, Ltd., Oxford, 2004, pp. 40–58.
11 P. E. Ebong, D. U. Owu and E. U. Isong, *Plant Foods Hum. Nutr.*, 1999, **53**, 209–222.
12 R. H. Müller, W. Mehnert, J. S. Lucks, C. Schwarz, A. zur Mühlen, H. Weyhers, C. Freitas and D. Rühl, *Eur. J. Pharm. Biopharm.*, 1995, **41**, 62–69.
13 M. Trotta, F. Debernardi and O. Caputo, *Int. J. Pharm*, 2003, **257**, 153–160.
14 N. J. Krog and F. V. Sparso, Food emulsifiers: Their chemical and physical properties, in *Food emulsions*, ed. S. E. Friberg, K. Larsson and J. Sjöblom, New York, Marcel Dekker, 2004, pp. 45–91.
15 F. Snyder, *Progr. Chem. Fats Lipids*, 1969, **10**, 287–335.
16 F. M. Helmy and M. H. Hack, *Comp. Biochem. Physiol.*, 1967, **23**, 329–334.
17 F. Paltauf, H. Hauser and M. C. Phillips, *Biochim. Biophys. Acta*, 1971, **249**, 539–547.
18 D. Vollhardt and U. Gehlert, *Prog. Colloid Polym. Sci.*, 1994, **97**, 302–306.
19 D. Vollhardt and U. Gehlert, *Tenside Surfactant Deterg.*, 1996, **33**, 196–203.
20 W. Bauman and H. K. Mangold, *J. Org. Chem.*, 1964, **29**, 3055–3057.
21 F. Paltauf and A. Hermetter, *Methods Enzymol.*, 1991, **197**, 134.
22 S. Hénon and J. Meunier, *Rev. Sci. Instrum.*, 1991, **62**, 936–939.
23 D. Hönig and D. Möbius, *J. Phys. Chem.*, 1991, **95**, 4590–4592.
24 D. Vollhardt, *Curr. Opin. Colloid Interface Sci.*, 2014, **19**, 183–197.
25 J. Als Nielsen, F. Christensen and P. S. Pershan, *Phys. Rev. Lett.*, 1982, **48**, 1107–1111.
26 J. Als-Nielsen, D. Jacquemain, K. Kjaer, F. Leveiller, M. Lahav and L. Leiserowitz, *Phys. Rep.*, 1994, **246**, 251–313.
27 K. Kjaer, *Physica B*, 1994, **198**, 100–109.
28 D. Vollhardt and G. Brezesinski, in *Recent Progress in Colloid and Surface Chemistry with Biological Applications*, ed. C. Wang, *et al.*, ACS Symposium Series, American Chemical Society, Washington, DC, 2015, pp. 377–419.
29 F. Bringezu, B. Dobner and G. Brezesinski, *Chem. – Eur. J.*, 2002, **8**, 3203–3210.
30 A. M. Bibo and I. R. Peterson, *Adv. Mater.*, 1990, **2**, 309–311.
31 D. Vollhardt and G. Brezesinski, *Langmuir*, 2016, **32**, 7316–7325.
32 D. Vollhardt, N. Nandi and S. Dutta Banik, *Phys. Chem. Chem. Phys.*, 2011, **13**, 4812–4829.
33 N. Nandi, D. Vollhardt and G. Brezesinski, *J. Phys. Chem. B*, 2004, **108**, 327–335.